

**Epigenetic silencing by the HUSH complex mediates position-effect variegation in human cells**

Iva A. Tchakovnikarova<sup>1†</sup>, Richard T. Timms<sup>1†</sup>, Nicholas J. Matheson<sup>1</sup>, Kim Wals<sup>1</sup>, Robin Antrobus<sup>1</sup>, Berthold Göttgens<sup>2</sup>, Gordon Dougan<sup>3</sup>, Mark A. Dawson<sup>4</sup>, Paul J. Lehner<sup>1\*</sup>

<sup>1</sup>Department of Medicine and <sup>2</sup>Department of Haematology, Cambridge Institute for Medical Research, Addenbrooke's Hospital, Hills Road, Cambridge, CB2 0XY, UK

<sup>3</sup>Wellcome Trust Sanger Institute, Wellcome Trust Genome Campus, Cambridge, CB10 1SA, UK

<sup>4</sup>Peter MacCallum Cancer Centre, St Andrews Place, East Melbourne, Victoria 3002, Australia

<sup>†</sup>These authors contributed equally to the work.

**Abstract:**

Forward genetic screens in *Drosophila melanogaster* for modifiers of position-effect variegation have revealed the basis of much of our understanding of heterochromatin. We took an analogous approach to identify genes required for epigenetic repression in human cells. A non-lethal forward genetic screen in near-haploid KBM7 cells identified the Human Silencing Hub (HUSH), a complex of three poorly-characterised proteins, TASOR, MPP8, and periphilin, which is absent from *Drosophila* but conserved from fish to humans. We suggest that the HUSH complex is recruited to genomic loci rich in H3K9me3, where subsequent recruitment of the methyltransferase SETDB1 is required for H3K9me3 deposition and transcriptional silencing. Loss of HUSH components resulted in decreased H3K9me3 at endogenous genomic loci and altered transcription, as well as derepression of retroviruses integrated into heterochromatin.

## **Main text:**

The positioning of a normally active gene into heterochromatin can result in epigenetic silencing, a phenomenon known as position-effect variegation (PEV) (1). Forward genetic screens in the fruit fly *Drosophila melanogaster* for mutations that act as suppressors or enhancers of PEV have identified a range of key regulators of heterochromatin (2). These include heterochromatin protein 1 (HP1) (3) and Su(var)3-9 (4), which respectively bind and deposit the key repressive histone modification, tri-methylated lysine 9 of histone H3 (H3K9me3) (5, 6). Here we set out to identify genes involved in PEV in human cells, using an analogous forward genetic screen in the haploid human KBM7 cell line.

We transduced KBM7 cells with a lentiviral construct encoding a green fluorescent protein (GFP) fusion protein driven by the spleen focus-forming virus (SFFV) promoter (Fig. 1A). Whilst the majority of transduced cells displayed high GFP expression, ~20% of the cells exhibited lower GFP expression (Fig. 1B). This was likely to be a result of reporter integration into a repressive chromatin environment. To identify the genes required for this epigenetic suppression, we isolated the population of GFP<sup>dim</sup> cells by fluorescence-activated cell sorting (FACS), mutagenised them with a gene-trap retrovirus, and enriched for rare mutant GFP<sup>bright</sup> cells via two rounds of FACS (Fig. 1C). Mapping the gene-trap integration sites among the GFP<sup>bright</sup> cells identified several genes that were significantly enriched for inactivating insertions compared to an unselected control population, including *SETDB1*, *FAM208A*, *MPHOSPH8* (encoding M-phase phosphoprotein 8, MPP8) and *PPHLN1* (encoding periphilin) (Fig. 1D and fig. S1A). The uncharacterised gene *FAM208A* was renamed **TASOR (Transgene Activation Suppressor)**.

We validated the role of these four genes by short-hairpin RNA (shRNA)-mediated knockdown in KBM7 cells (fig. S1, B and C), and using an independent GFP reporter

construct in HeLa cells (Fig. 1E and fig. S2). This effect was not limited to retroviral constructs, as stably integrated reporter constructs delivered by transfection were similarly repressed (Fig. 1F and fig. S3), and was apparent using both viral and cellular promoters (fig. S4). The variable proportion of GFP<sup>dim</sup> cells observed with different reporter constructs, however, did suggest that the DNA sequence of the reporter may influence the degree of silencing. Thus, repression by these four genes appeared to be predominantly governed by the genomic landscape surrounding the transgene integration site, but could also be modulated by the sequence composition of the reporter.

To determine whether these genes act as part of a multi-protein complex, we analysed TASOR immunoprecipitates from KBM7 nuclei by mass spectrometry. After discounting proteins also present in control immunoprecipitates, two putative interacting proteins remained: MPP8 and periphilin (table S1 and fig. S5A), the same proteins identified by our genetic screen (Fig. 1D). Thus, both genetic and proteomic approaches converged on a repressive complex comprising TASOR, MPP8 and periphilin, which we named the **Human Silencing Hub (HUSH)** complex (fig. S5B). TASOR, MPP8 and periphilin all localised to the nucleus (fig. S5, C and D). Interactions between HUSH complex members were readily confirmed by co-immunoprecipitation experiments (Fig. 1G), and knockdown of each of the three proteins resulted in decreased levels of the other HUSH complex subunits (fig. S5, E and F). This was not the case upon knockdown of SETDB1 (fig. S5G), which did not appear to be a constitutive member of the HUSH complex.

As the leading hit in the genetic screen was the H3K9 methyltransferase SETDB1 (7), and the chromodomain of MPP8 binds H3K9me3 (8–10), our investigation into the mechanism of repression by the HUSH complex focussed on the repressive H3K9me3 histone mark. High levels of H3K9me3 were found on repressed, GFP<sup>dim</sup> reporters, but not on active, GFP<sup>bright</sup> reporters (Fig. 2A and fig. S6). Consistent with a role for the HUSH complex

in facilitating the deposition of H3K9me3, depletion of HUSH subunits resulted in a decrease in H3K9me3 across the reporter (Fig. 2B), concomitant with an increase in GFP mRNA expression (Fig. 2C). Furthermore, HUSH subunits were chromatin-associated (Fig. 2D), and we detected binding of epitope-tagged HUSH subunits to a repressed reporter (Fig. 2E). HUSH subunits co-immunoprecipitated with SETDB1 (Fig. 2F), and knockdown of HUSH complex members impaired the recruitment of SETDB1 to a repressed GFP reporter (Fig. 2G). Thus, the HUSH complex appeared to facilitate the deposition of the repressive H3K9me3 histone modification through the targeted recruitment of SETDB1.

HUSH repressed almost all GFP<sup>dim</sup> reporter integrations (Fig. 3A and fig. S7). Thus, by comparing the integration sites of the GFP reporter in the GFP<sup>dim</sup> versus the GFP<sup>bright</sup> populations, we could determine where HUSH acted in the genome (Fig. 3B). GFP<sup>dim</sup> integrations were most enriched in proximity to H3K9me3, and underrepresented in proximity to histone marks correlated with active chromatin (Fig. 3C and fig. S8A). We also compared genes which were highly enriched for GFP<sup>dim</sup> insertions over GFP<sup>bright</sup> insertions (“dim genes”) or vice versa (“bright genes”). H3K9me3 levels across “dim genes” were much higher than across “bright genes” (Fig. 3D and fig. S8B). The majority of the leading “dim genes” were KRAB-ZNF genes (fig. S8, C to E), which are covered with high levels of H3K9me3 (11), deposited by SETDB1 (12). To validate these observations directly, we used the CRISPR/Cas9 system to integrate a non-retroviral GFP reporter construct at an example KRAB-ZNF gene (Fig. 3E). This construct was indeed subject to HUSH-mediated repression (Fig. 3F and fig. S9). Thus, the HUSH complex preferentially silenced transgenes integrating into chromatin marked by high levels of H3K9me3.

Recruitment of the HUSH complex to loci rich in H3K9me3 could be mediated through the chromodomain of MPP8 (8–10). An H3 peptide trimethylated at K9, but not an unmodified H3 peptide, pulled-down MPP8 together with TASOR from a nuclear lysate (fig.

S10A). TASOR recruitment to H3K9me3 was dependent on MPP8, and was lost following MPP8 depletion (fig. S10A). Additionally, the purified chromodomain of MPP8 has been shown to bind chromatin marked by high levels of H3K9me3 (fig. S10B) (13), and we detected binding of epitope-tagged HUSH subunits to genes rich in H3K9me3 (fig. S10C). To determine whether the chromodomain of MPP8 was essential for re-establishment of reporter repression, we generated a HUSH triple knockout reporter clone lacking expression of TASOR, MPP8 and periphilin using CRISPR/Cas9 technology (fig. S11). Re-expression of wild-type HUSH subunits resulted in re-repression of the reporter, but this was severely abrogated upon reconstitution with an MPP8 chromodomain mutant (W80A) that cannot bind H3K9me3 (8) (Fig. 3G and fig. S12A). In contrast, in cells lacking MPP8 alone, a functional chromodomain was not absolutely critical for re-repression of the reporter, as the W80A MPP8 mutant could partially restore reporter repression (fig. S12, B and C). This result suggested that another member of the HUSH complex must also contribute to HUSH localisation at target sites. Indeed we found that, in the absence of either TASOR or MPP8, periphilin was still able to localise to chromatin (fig. S12, D and E). Thus, the chromodomain of MPP8 was required for the initial targeting of the HUSH complex to H3K9me3-marked loci, but periphilin also contributed to the maintenance of the complex at chromatin.

Given that the HUSH complex regulates H3K9me3 levels across integrated reporter constructs, we asked whether it maintains H3K9me3 at endogenous genomic loci. ChIP followed by deep sequencing (ChIP-seq) in CRISPR/Cas9-generated TASOR, MPP8, periphilin and SETDB1 knockout HeLa cells (fig. S11) identified 918 shared genomic loci (14) with markedly reduced levels of H3K9me3 upon loss of HUSH subunits (Fig. 4A and table S2). Furthermore, knockout of SETDB1 resulted in a decrease in H3K9me3 at 916/918 (99.6%) of the shared loci affected by loss of HUSH, with the majority (91%) showing a >3-fold reduction (Fig. 4B). This confirmed a functional association between this critical

methyltransferase and the HUSH complex. At four example loci, the decrease in H3K9me3 levels as a result of loss of HUSH or SETDB1 (Fig. 4C) resulted in modest increases in gene expression (Fig. 4D).

Retroviral integration into heterochromatin is a natural mimic of position effect variegation. As such we reasoned that viruses – and not merely transgenes delivered in the context of self-inactivating (SIN) vectors – might also be subject to HUSH-mediated repression. We infected the CD4<sup>+</sup> lymphoid cell line Jurkat with a standard HIV-1 reporter virus which contains the wild-type HIV-1 LTR promoter driving both the HIV-1 transactivator Tat and GFP (HIV-1 LTR-Tat-IRES-GFP) (15) (Fig. 4E). Again we observed a range of GFP expression levels (Fig. 4F). The repressed proviruses in the GFP<sup>dim</sup> cells were subject to HUSH-mediated repression, because knockdown of HUSH subunits resulted in transcriptional activation (Fig. 4G) accompanied by a decrease in H3K9me3 levels (Fig. 4H). Depletion of HUSH subunits also resulted in derepression of silent HIV-1 reporter proviruses in J-Lat clones (fig. S13), a widely used cellular model of HIV-1 silencing (15, 16), and similarly in an analogous “K-Lat” model that we generated in KBM7 cells (fig. S14). This effect was not limited to the HIV-1 LTR; we also found HUSH acted upon repressed murine leukaemia virus (MLV) integrations (fig. S15). Thus the HUSH complex mediates epigenetic regulation of both endogenous and viral genes at heterochromatic loci marked by H3K9me3.

By replicating a classic *Drosophila* forward genetic screen for modifiers of PEV in cultured human cells, we identified the HUSH complex. HUSH mediated epigenetic repression through the recruitment of SETDB1 and the deposition of H3K9me3. Surprisingly we did not identify a role for canonical heterochromatin regulators required for PEV in *Drosophila*, such as HP1 (fig. S16) (17). HUSH complex subunits are absent from *Drosophila* but conserved from fish to humans, suggesting an additional, more recently acquired route to H3K9me3-mediated heterochromatin regulation in mammalian cells.

## **References and Notes:**

1. G. Schotta, A. Ebert, R. Dorn, G. Reuter, Position-effect variegation and the genetic dissection of chromatin regulation in *Drosophila*. *Semin. Cell Dev. Biol.* **14**, 67–75 (2003).
2. S. C. R. Elgin, G. Reuter, Position-effect variegation, heterochromatin formation, and gene silencing in *Drosophila*. *Cold Spring Harb. Perspect. Biol.* **5**, a017780 (2013).
3. T. C. James, S. C. Elgin, Identification of a nonhistone chromosomal protein associated with heterochromatin in *Drosophila melanogaster* and its gene. *Mol. Cell. Biol.* **6**, 3862–72 (1986).
4. G. Reuter, R. Dorn, G. Wustmann, B. Friede, G. Rauh, Third chromosome suppressor of position-effect variegation loci in *Drosophila melanogaster*. *MGG Mol. Gen. Genet.* **202**, 481–487 (1986).
5. S. Rea *et al.*, Regulation of chromatin structure by site-specific histone H3 methyltransferases. *Nature.* **406**, 593–9 (2000).
6. A. J. Bannister *et al.*, Selective recognition of methylated lysine 9 on histone H3 by the HP1 chromo domain. *Nature.* **410**, 120–4 (2001).
7. D. C. Schultz, K. Ayyanathan, D. Negorev, G. G. Maul, F. J. Rauscher, SETDB1: a novel KAP-1-associated histone H3, lysine 9-specific methyltransferase that contributes to HP1-mediated silencing of euchromatic genes by KRAB zinc-finger proteins. *Genes Dev.* **16**, 919–32 (2002).
8. K. Kokura, L. Sun, M. T. Bedford, J. Fang, Methyl-H3K9-binding protein MPP8 mediates E-cadherin gene silencing and promotes tumour cell motility and invasion. *EMBO J.* **29**, 3673–87 (2010).
9. Y. Chang, J. R. Horton, M. T. Bedford, X. Zhang, X. Cheng, Structural insights for MPP8 chromodomain interaction with histone H3 lysine 9: potential effect of phosphorylation on methyl-lysine binding. *J. Mol. Biol.* **408**, 807–14 (2011).
10. J. Li *et al.*, Structural basis for specific binding of human MPP8 chromodomain to histone H3 methylated at lysine 9. *PLoS One.* **6**, e25104 (2011).
11. H. O’Geen *et al.*, Genome-wide analysis of KAP1 binding suggests autoregulation of KRAB-ZNFs. *PLoS Genet.* **3**, e89 (2007).
12. S. Fietze, H. O’Geen, K. R. Blahnik, V. X. Jin, P. J. Farnham, ZNF274 recruits the histone methyltransferase SETDB1 to the 3’ ends of ZNF genes. *PLoS One.* **5**, e15082 (2010).
13. G. Kungulovski *et al.*, Application of histone modification-specific interaction domains as an alternative to antibodies. *Genome Res.* **24**, 1842–53 (2014).

14. Materials and methods are available as supplementary materials on *Science Online*.
15. A. Jordan, P. Defechereux, E. Verdin, The site of HIV-1 integration in the human genome determines basal transcriptional activity and response to Tat transactivation. *EMBO J.* **20**, 1726–38 (2001).
16. A. Jordan, D. Bisgrove, E. Verdin, HIV reproducibly establishes a latent infection after acute infection of T cells in vitro. *EMBO J.* **22**, 1868–77 (2003).
17. J. C. Eissenberg *et al.*, Mutation in a heterochromatin-specific chromosomal protein is associated with suppression of position-effect variegation in *Drosophila melanogaster*. *Proc. Natl. Acad. Sci. U. S. A.* **87**, 9923–7 (1990).
18. E. J. Duh, W. J. Maury, T. M. Folks, A. S. Fauci, A. B. Rabson, Tumor necrosis factor alpha activates human immunodeficiency virus type 1 through induction of nuclear factor binding to the NF-kappa B sites in the long terminal repeat. *Proc. Natl. Acad. Sci. U. S. A.* **86**, 5974–8 (1989).
19. C. Demaison *et al.*, High-level transduction and gene expression in hematopoietic repopulating cells using a human immunodeficiency [correction of immunodeficiency] virus type 1-based lentiviral vector containing an internal spleen focus forming virus promoter. *Hum. Gene Ther.* **13**, 803–13 (2002).
20. L. M. Duncan *et al.*, Fluorescence-based phenotypic selection allows forward genetic screens in haploid human cells. *PLoS One.* **7**, e39651 (2012).
21. R. T. Timms *et al.*, Haploid genetic screens identify an essential role for PLP2 in the downregulation of novel plasma membrane targets by viral E3 ubiquitin ligases. *PLoS Pathog.* **9**, e1003772 (2013).
22. J. E. Carette *et al.*, Global gene disruption in human cells to assign genes to phenotypes by deep sequencing. *Nat. Biotechnol.* **29**, 542–6 (2011).
23. B. Langmead, S. L. Salzberg, Fast gapped-read alignment with Bowtie 2. *Nat. Methods.* **9**, 357–9 (2012).
24. F. A. Ran *et al.*, Genome engineering using the CRISPR-Cas9 system. *Nat. Protoc.* **8**, 2281–308 (2013).
25. M. A. Dawson *et al.*, JAK2 phosphorylates histone H3Y41 and excludes HP1alpha from chromatin. *Nature.* **461**, 819–22 (2009).
26. N. K. Wilson *et al.*, Combinatorial transcriptional control in blood stem/progenitor cells: genome-wide analysis of ten major transcriptional regulators. *Cell Stem Cell.* **7**, 532–44 (2010).
27. S. K. Harten *et al.*, The first mouse mutants of D14Abb1e (Fam208a) show that it is critical for early development. *Mamm. Genome* (2014), doi:10.1007/s00335-014-9516-0.

28. M. Kurita, H. Suzuki, Y. Kawano, S. Aiso, M. Matsuoka, CR/periphilin is a transcriptional co-repressor involved in cell cycle progression. *Biochem. Biophys. Res. Commun.* **364**, 930–6 (2007).
29. M. Kurita *et al.*, Overexpression of CR/periphilin downregulates Cdc7 expression and induces S-phase arrest. *Biochem. Biophys. Res. Commun.* **324**, 554–61 (2004).
30. A. S. Soehn *et al.*, Periphilin is strongly expressed in the murine nervous system and is indispensable for murine development. *Genesis.* **47**, 697–707 (2009).

### **Acknowledgements:**

We thank J. Sinclair, L. Dölken, A. Schuldt, N. Wilson and F. Calero-Nieto for helpful discussion. We are indebted to R. Schulte and his team for FACS, M. Gratian, M. Bowen and K. Jayawardena (CIMR); N. Smerdon (Wellcome Trust Sanger Institute); and S. Andrews (Babraham Institute) for SeqMonk customisation. This work was supported by a Wellcome Trust Principal Research Fellowship to P.J.L. (084957/Z/08/Z) and studentship to I.A.T., an MRC Centenary Award to R.T.T., and the Cambridge Biomedical Research Centre (UK). The CIMR is in receipt of a Wellcome Trust Strategic Award. Raw sequence data is archived at GEO (GSE60056 and GSE63116) and SRA (PRJNA257239).

## **Figure Captions:**

**Fig. 1. A haploid genetic screen identifies a requirement for the HUSH complex for epigenetic repression in human cells.**

(A) Schematic view of the GFP reporter construct (see (14) for further details). (B) Transduction of KBM7 cells with the GFP reporter results in a majority GFP<sup>bright</sup> population plus a repressed GFP<sup>dim</sup> population. (C) A haploid genetic screen to identify genes required for repression of the GFP reporter. (D) Bubble plot illustrating the hits from the screen. Bubble size is proportional to the number of independent inactivating gene-trap integrations identified (shown in brackets). (E and F) Validation of the screen hits in HeLa cells, using an independent lentiviral reporter (E) and a non-viral reporter containing the phosphoglycerate kinase 1 (PGK) promoter driving GFP delivered by transfection (F). Histograms were gated on GFP<sup>+</sup> cells. (G) TASOR, MPP8 and periphilin form a complex. Endogenous TASOR, MPP8 and periphilin were immunoprecipitated from KBM7 cells, and the indicated co-immunoprecipitating proteins identified by immunoblot. We were unable to blot for periphilin as the antibody does not recognise its epitope following NP-40 lysis.

**Fig. 2. The HUSH complex functions through H3K9me3 via the targeted recruitment of SETDB1.**

(A) GFP<sup>dim</sup> integrations are marked by H3K9me3 but not H3K27me3. H3K9me3 and H3K27me3 levels across the reporter were assessed by ChIP-qPCR in sorted GFP<sup>dim</sup> and GFP<sup>bright</sup> populations. (B and C) Knockdown of HUSH components results in a loss of H3K9me3 across a GFP<sup>dim</sup> reporter as assessed by ChIP-qPCR (B), concomitant with an increase in GFP transcript levels (C). (D) Subcellular fractionation showing that HUSH subunits are found in the chromatin fraction. GAPDH, Rb and HP1 $\alpha$  were used to validate the fractionation. (E) V5-tagged HUSH subunits bind to a repressed GFP reporter as assessed by ChIP-qPCR. (F) Co-immunoprecipitation of TASOR and MPP8 with SETDB1. (G) Knockdown of HUSH components results in impaired recruitment of SETDB1 to a GFP<sup>dim</sup> reporter, as assessed by ChIP-qPCR.

**Fig. 3. The HUSH complex functions at genomic loci rich in H3K9me3.**

(A) HUSH represses the majority of GFP<sup>dim</sup> reporter integrations. Populations of GFP<sup>dim</sup> and GFP<sup>bright</sup> cells were isolated by FACS and subjected to knockdown of TASOR. (B to D) The HUSH complex acts at genomic loci marked by high levels of H3K9me3. Reporter integration sites were mapped among the GFP<sup>dim</sup> and GFP<sup>bright</sup> populations (B). Correlating integration sites with ENCODE ChIP-seq peaks for K562 cells showed that GFP<sup>dim</sup> integration sites were most enriched in proximity to H3K9me3 (C). Examples of the top “dim genes” and “bright genes” are shown in (D). (E and F) HUSH-mediated repression of a GFP reporter construct targeted to ZNF594. (G) Re-establishment of reporter repression upon reconstitution of a HUSH triple knockout clone.

**Fig. 4. The HUSH complex maintains H3K9me3 at endogenous loci and represses viruses integrated into heterochromatin.**

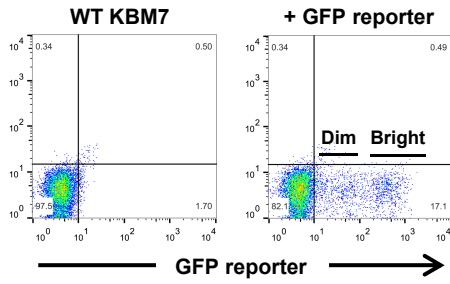
(A to C) Loss of HUSH results in decreased H3K9me3 at endogenous genomic loci. Global levels of H3K9me3 were measured by ChIP-seq in wild-type HeLa cells and cells lacking HUSH subunits and SETDB1. The CRISPR/Cas9-mediated disruption of TASOR, MPP8 and periphilin resulted in decreased H3K9me3 at shared loci (A). Knockout of SETDB1 resulted in decreased H3K9me3 at over 99% of these loci, with the majority (91%) showing a >3-fold reduction (B). Four example loci are shown in (C). (D) Loss of HUSH resulted in increased expression of the four example genes from (C), as measured by qRT-PCR. (E to H) Proviral repression by the HUSH complex. Schematic view of the HIV-1 LTR-Tat-IRES-GFP virus (E). Infection of Jurkat cells resulted in a range of GFP expression levels (F); the proviruses in the GFP<sup>dim</sup> cells were repressed by the HUSH complex (G) through H3K9me3 (H). TNF- $\alpha$  activates transcription from the HIV-1 LTR through the NF- $\kappa$ B pathway (18).

# Revised Figure 1

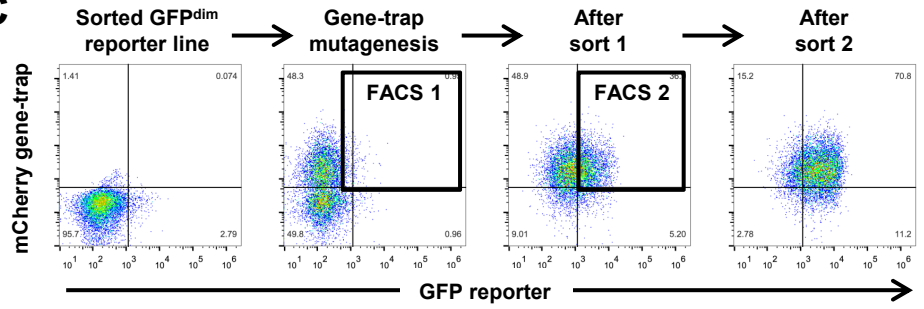
**A**



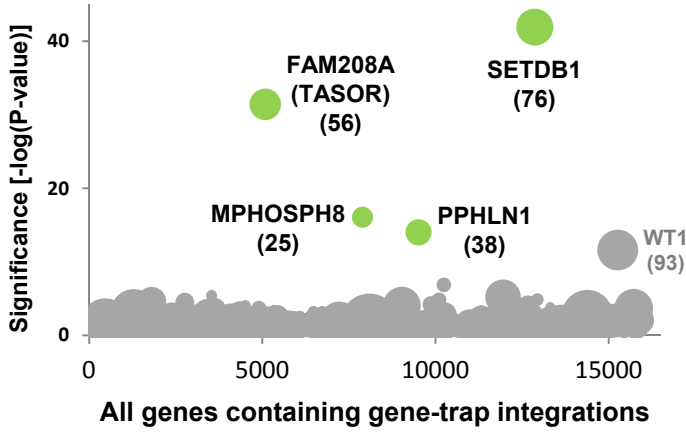
**B**



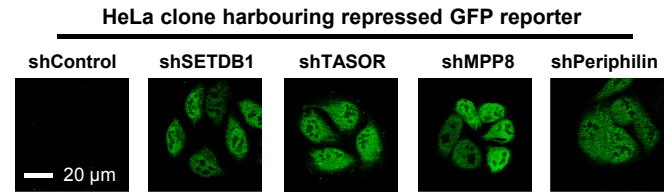
**C**



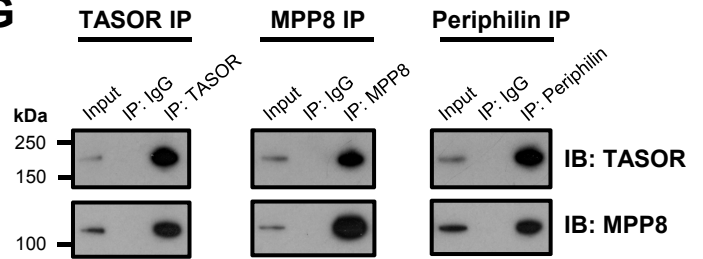
**D**



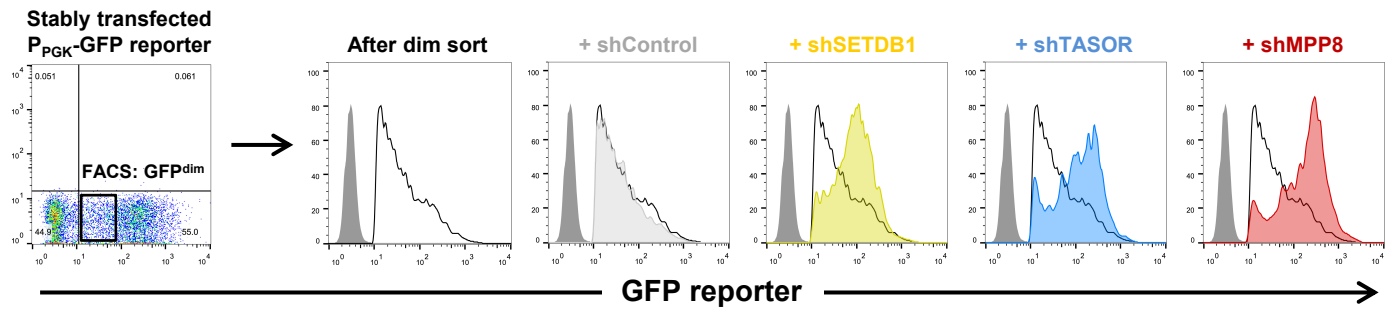
**E**



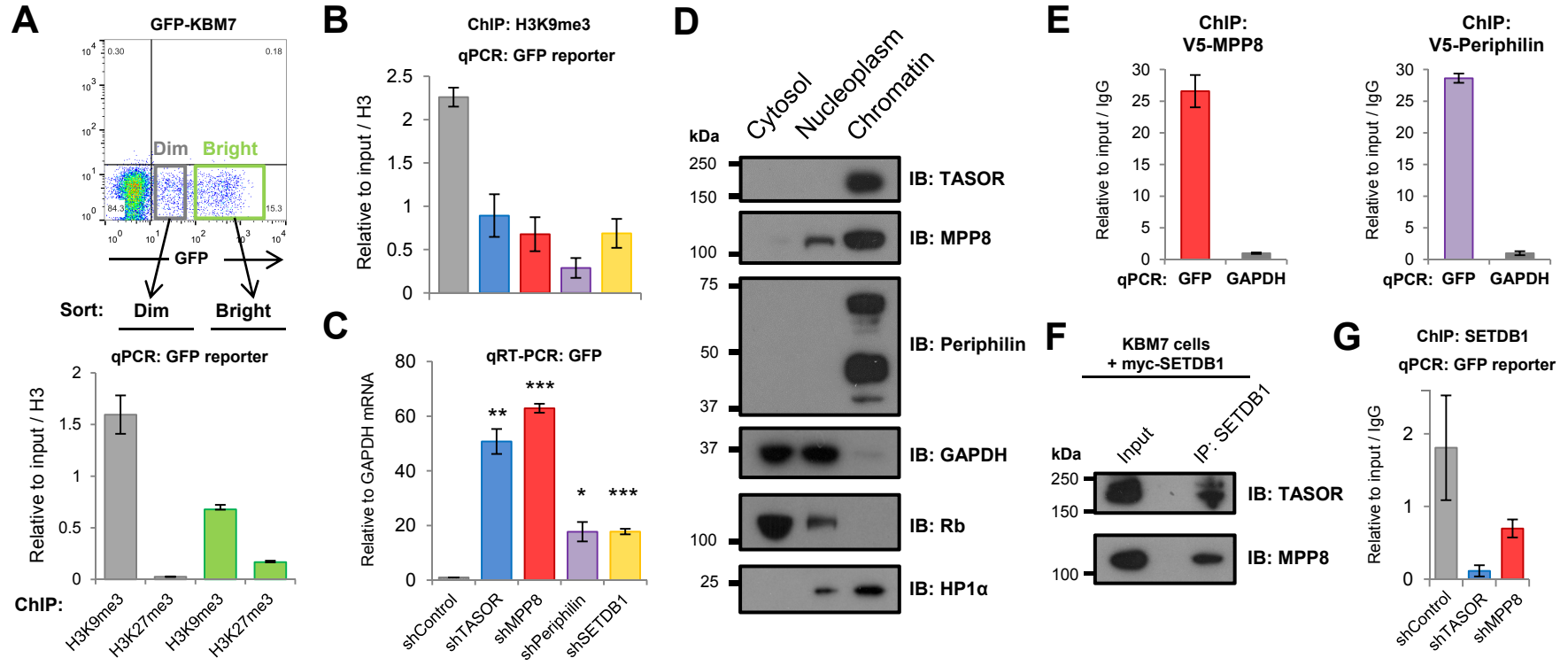
**G**



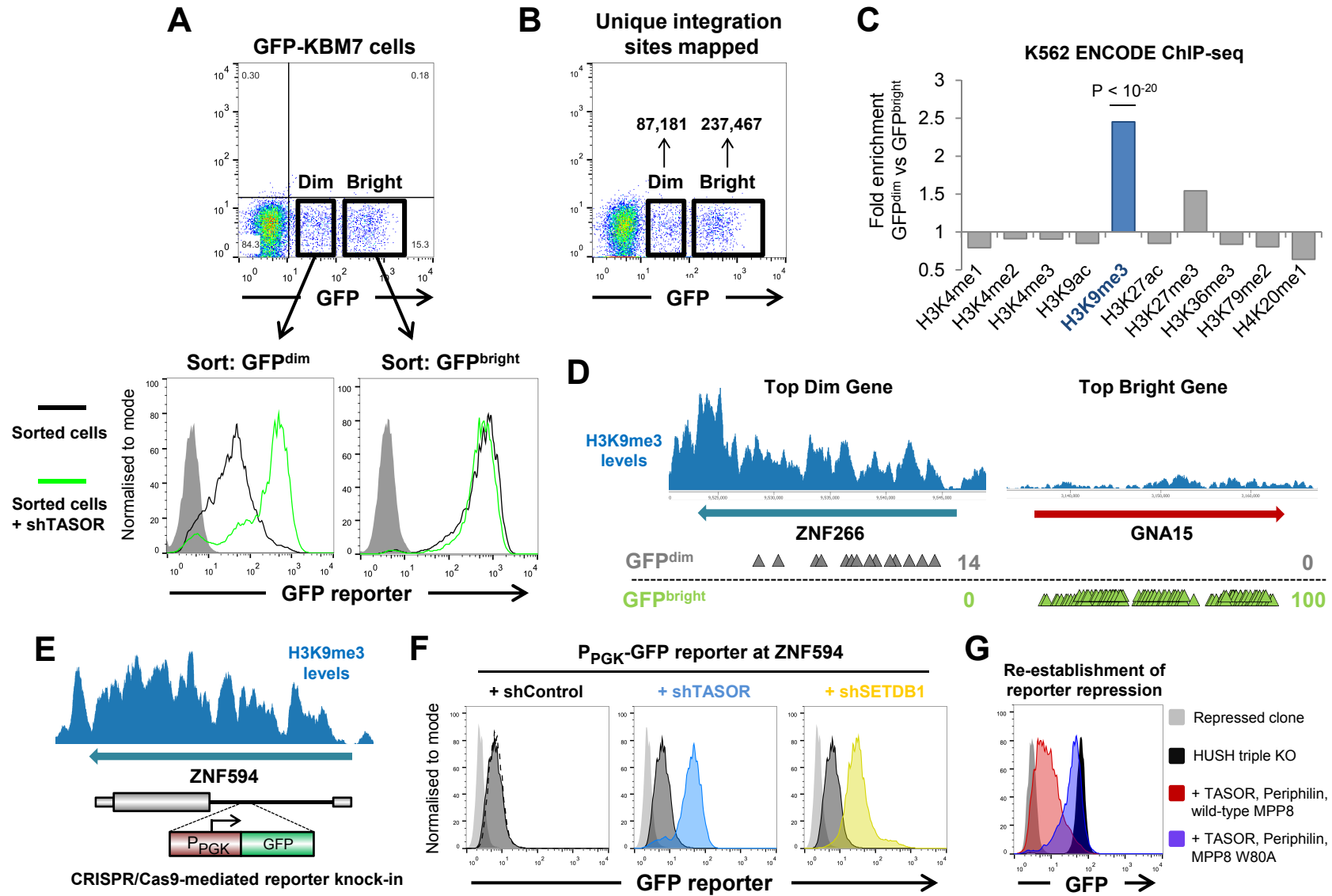
**F**



# Revised Figure 2



# Revised Figure 3



# Revised Figure 4

